CARBON CYCLE

Enhanced seasonal CO_2 exchange caused by amplified plant productivity in northern ecosystems

Matthias Forkel,[1*†] Nuno Carvalhais,[1,2*] Christian Rödenbeck,[1] Ralph Keeling,[3] Martin Heimann,[1,4] Kirsten Thonicke,[5] Sönke Zaehle,[1] Markus Reichstein[1,6]

Atmospheric monitoring of high northern latitudes (above 40°N) has shown an enhanced seasonal cycle of carbon dioxide (CO_2) since the 1960s, but the underlying mechanisms are not yet fully understood. The much stronger increase in high latitudes relative to low ones suggests that northern ecosystems are experiencing large changes in vegetation and carbon cycle dynamics. We found that the latitudinal gradient of the increasing CO_2 amplitude is mainly driven by positive trends in photosynthetic carbon uptake caused by recent climate change and mediated by changing vegetation cover in northern ecosystems. Our results underscore the importance of climate–vegetation–carbon cycle feedbacks at high latitudes; moreover, they indicate that in recent decades, photosynthetic carbon uptake has reacted much more strongly to warming than have carbon release processes.

The seasonal cycle of atmospheric carbon dioxide (CO_2) in the Northern Hemisphere is mainly controlled by carbon uptake and release processes of the land biosphere (*1*), specifically by the difference between photosynthetic carbon uptake [gross primary production (GPP)] and ecosystem respiration (Reco) (*2*). Airborne and surface data show that the amplitude of the seasonal cycle (henceforth "CO_2 amplitude") has increased since 1960, particularly north of 45°N, where increases as large as 50% have occurred (*1*–*4*). The strong seasonality of GPP and Reco in northern land ecosystems causes a larger average CO_2 amplitude in high northern latitudes than in low ones (*2*, *5*). The larger trends in CO_2 amplitude at higher latitudes consequently imply that they are caused by changing carbon cycle dynamics in northern ecosystems (*4*).

A variety of factors may contribute to the CO_2 amplitude trend. Arctic and boreal regions have experienced strong warming in recent decades (*6*), and a "greening" trend has been detected from satellites, indicating enhanced plant growth (*7*, *8*) (Fig. 1, A and B). These satellite observations are confirmed by ground observations showing increases in shrub coverage in the tundra (*9*), tree growth along the tundra–boreal forest transition zone (*10*), and deciduous tree cover from recovery after severe boreal forest fires (*11*). Additionally, various estimates show positive trends in both annual amplitudes and annual totals of GPP (*12*, *13*) and in net biome productivity (NBP) (*14*) in northern ecosystems (Fig. 1, C and D). The intensification of agriculture in the mid-latitudes also likely contributes to the CO_2 amplitude trends (*15*, *16*). These multiple observational signals point to amplified plant productivity as a likely cause of the increase in CO_2 amplitude (*1*, *3*, *7*, *17*). Nonetheless, a quantitative explanation of the amplitude trends is still lacking. Current Earth system models consistently underestimate the CO_2 amplitude trend (*4*) and its gradient with latitude, which suggests that these models are missing or underrepresenting key processes (*18*).

Here, we examined the cause of the CO_2 amplitude increase by combining observations from long-term monitoring sites of atmospheric CO_2 concentration, satellite observation of vegetation greenness (*19*), and global observation-based data sets of GPP (*12*) and NBP (*14*) with results from the LPJmL dynamic global vegetation model (*20*, *21*) coupled with the TM3 atmospheric transport model (*22*) [hereinafter called LPJmL+TM3 (*23*)] to explain the observed latitudinal gradient of CO_2 amplitude trends. Unlike other biosphere models that were previously evaluated against CO_2 amplitude trends (*4*), LPJmL considers several processes that potentially contribute to a better explanation of these trends, including agriculture, irrigation, and land use change (*21*); vegetation dynamics; and processes that control northern vegetation dynamics, such as permafrost (*24*) and fire (*25*) driven by observed burned-area data (*26*). Moreover, LPJmL uses an improved phenology module (*26*) that has been optimized against satellite observations of FAPAR (fraction of absorbed photosynthetic active radiation), albedo, and an observation-based data set of GPP, resulting in a better representation of climate controls on vegetation dynamics as well as global carbon fluxes and stocks (*26*, *27*). Note that atmospheric CO_2 data were not used to constrain LPJmL.

We estimated CO_2 amplitude trends in observed time series at 19 monitoring sites with at least 20 years of data (table S1). We found much stronger positive CO_2 amplitude trends at high-latitude sites [e.g., 0.08 ppm year^{-1} ≈ 0.53% year^{-1} at Point Barrow (BRW) during 1971–2011] than at low-latitude sites [e.g., 0.005 ppm year^{-1} ≈ 0.076% year^{-1} at Mauna Loa (MLO) during 1970–2011] (Fig. 1E). These estimated trends were similar to those of previous studies (*2*, *4*) with small differences due to station selection, time series analysis methods, and time series length. We found weaker trends in the CO_2 amplitude, especially at MLO, because this trend originates mostly from low CO_2 amplitude values in the 1960s and weakens from 1970 onward. To account for the effect of time series length, we estimated the uncertainties in CO_2 amplitude trends by computing trends for different combinations of start and end years (fig. S1). The estimated uncertainties ($0.53_{0.39}^{0.64}$% year^{-1} at BRW, $0.076_{-0.059}^{0.19}$% year^{-1} at MLO, $50_{2.5}^{97.5}$percentiles of trend slope ensemble) demonstrate that only high-latitude sites have persistent long-term increases in CO_2 amplitude.

In comparison to surface-level site observations, LPJmL+TM3 had stronger CO_2 amplitude trends on average (Fig. 2A and table S2). However, LPJmL+TM3 reproduced the observed changes in CO_2 amplitude at higher atmospheric levels (fig. S2). LPJmL+TM3 simulations were well correlated with site observations regarding spatial patterns of mean CO_2 amplitude values (r = 0.84) and trends (r = 0.51, $P \leq 0.05$) (fig. S3). LPJmL+TM3 had a modest performance in representing the year-to-year variability of the CO_2 amplitude at some sites (*23*), which may indicate the importance of the effect of regional extreme events on the land carbon balances (*28*). LPJmL+TM3 reproduced the observed pattern of strong positive CO_2 amplitude trends north of 45°N, the large variability of trends in the mid-latitudes, and the small or nonsignificant trends south of 20°N. We found that simulations of CO_2 amplitudes were sensitive to the choice of the meteorological forcing data set for the TM3 transport model (fig. S4A). Therefore, we propagated the uncertainty both from time series length and meteorological forcing to the overall uncertainty of simulated CO_2 amplitude trends for a more robust model evaluation. The interannual variability of ocean CO_2 uptake had no distinct contribution to CO_2 amplitude trends in comparison to a climatology of ocean uptake (fig. S4B). LPJmL yielded positive trends in annual maximum FAPAR in northern ecosystems that are in good agreement with satellite observations (*27*) and yielded increases in annual amplitudes and totals of GPP and NBP that agree with independent observation-based GPP and NBP estimates (Fig. 1, B to D, and fig. S5). Although the model does not fully account for trends in agricultural fertilizer usage, the simulated trends in GPP of agricultural regions are comparable to an independent

[1]Max Planck Institute for Biogeochemistry, 07745 Jena, Germany. [2]CENSE, Departamento de Ciências e Engenharia do Ambiente, Faculdade de Ciências e Tecnologia, Universidade NOVA de Lisboa, Caparica, Portugal. [3]Scripps Institution of Oceanography, La Jolla, CA 92093, USA. [4]Department of Physical Sciences, University of Helsinki, Helsinki, Finland. [5]Potsdam Institute for Climate Impact Research, 14473 Potsdam, Germany. [6]Michael-Stifel-Center Jena for Data-driven and Simulation Science, 07743 Jena, Germany.
***Corresponding author. E-mail: matthias.forkel@geo.tuwien.ac.at (M.F.); ncarval@bgc-jena.mpg.de (N.C.)** †Present address: Department of Geodesy and Geoinformation, Technische Universität Wien, 1040 Vienna, Austria.

estimate (fig. S7). This comparison of LPJmL simulations and independent data sets demonstrates an amplification of plant productivity in northern ecosystems.

We quantified the contribution of land NBP from different regions to CO_2 amplitude trends (table S5 and fig. S6B). NBP from boreal regions contributed 51% to the average CO_2 amplitude in the 1970s at high northern latitude sites (>45°N). In the 2000s, the contribution of boreal regions increased to 54%, corresponding to an annual increase of $0.35^{0.41}_{0.14}$% year^{-1}. The contribution of arctic NBP was 17% in the 1970s and increased by $0.18^{0.24}_{0.12}$% year^{-1}. NBP from global agricultural regions contributed 11% in the 1970s and increased by $0.14^{0.16}_{0.01}$% year^{-1}. Temperate and tropical regions made only minor contributions to the trends in CO_2 amplitude. However, only trends in the contribution of arctic and boreal NBP were significant (P = 0.03 and P = 0.01, respectively) at northern sites. At low-latitude sites (0° to 45°N), NBP from boreal regions still contributed dominantly to the increase in CO_2 amplitude with $0.46^{0.52}_{0.09}$% year^{-1} (P = 0.12), followed by NBP from agricultural regions with $0.17^{0.26}_{-0.21}$% year^{-1} (P = 0.37) and NBP from arctic regions with $0.14^{0.19}_{0.08}$% year^{-1} (P = 0.12). Therefore, boreal regions contributed approximately 57%, arctic regions 25%, and agricultural regions 17% to the overall CO_2 amplitude trend at northern-latitude sites (41%, 14%, and 20% at low-latitude sites, respectively). The agricultural contribution in LPJmL is within the ranges found in previous studies (*15*, *16*). Similar to (*4*), we found that fossil fuel emissions and ocean CO_2 exchange have little impact on the trends in CO_2 amplitude (table S5). Consistent with Graven *et al.* (*4*), LPJmL attributes a dominant role to boreal and arctic ecosystems in driving the CO_2 amplitude increase.

Both GPP and Reco can potentially contribute to the increasing CO_2 amplitude. We found stronger trends in annual total GPP ($0.065^{0.083}_{0.053}$ PgC year^{-2}, LPJmL during 1970–2011) than in annual total Reco ($0.061^{0.07}_{0.051}$ PgC year^{-2}, LPJmL during 1970–2011) in northern ecosystems (fig. S8) and stronger trends in the GPP than in Reco annual amplitudes across all northern latitudes (fig. S9). The contribution of GPP to the CO_2 amplitude increased by $2.3^{3.2}_{-0.1}$% year^{-1}, whereas the increasing Reco contributed to a decrease of the seasonal amplitude of $-1.5^{0.22}_{-2.24}$% year^{-1}. Consequently, given the opposite signs of GPP and Reco fluxes, the effect of GPP on the CO_2 amplitude is attenuated but not compensated by Reco (table S5). This is consistent with earlier results (*29*) showing that the spatial variability of NEE and NBP amplitudes is strongly related to GPP. The stronger increase in GPP relative to Reco leads to a positive trend in northern ecosystem NBP of $0.011^{0.017}_{0.006}$ PgC year^{-2} (LPJmL), which is confirmed by independent estimates from the Jena CO_2 inversion scheme [$0.014^{0.02}_{0.0086}$ PgC year^{-2}, version s81_v3.6 (*14*)] (fig. S10). Trends in annual total GPP in northern ecosystems and CO_2 amplitude trends at northern-latitude sites show a strong linear relation across different LPJmL+TM3 model experiments (r^2 = 0.96; Fig. 3 and fig. S11). For example, an increase in CO_2 amplitude of 0.08 ppm year^{-1} at BRW requires an increase in boreal and arctic GPP of 0.07 PgC year^{-2}. Thus, the increase in the seasonal CO_2 amplitude can be explained by a photosynthesis-driven increase in net carbon uptake of northern ecosystems.

Several factors can contribute to the increased photosynthetic carbon uptake and hence to the latitudinal gradient of the increasing CO_2 amplitude. Rising atmospheric CO_2 and climate change directly affect physiological processes that can enhance photosynthesis (*30*). To test the relative effect of CO_2 fertilization and climate change on CO_2 amplitude trends, we performed

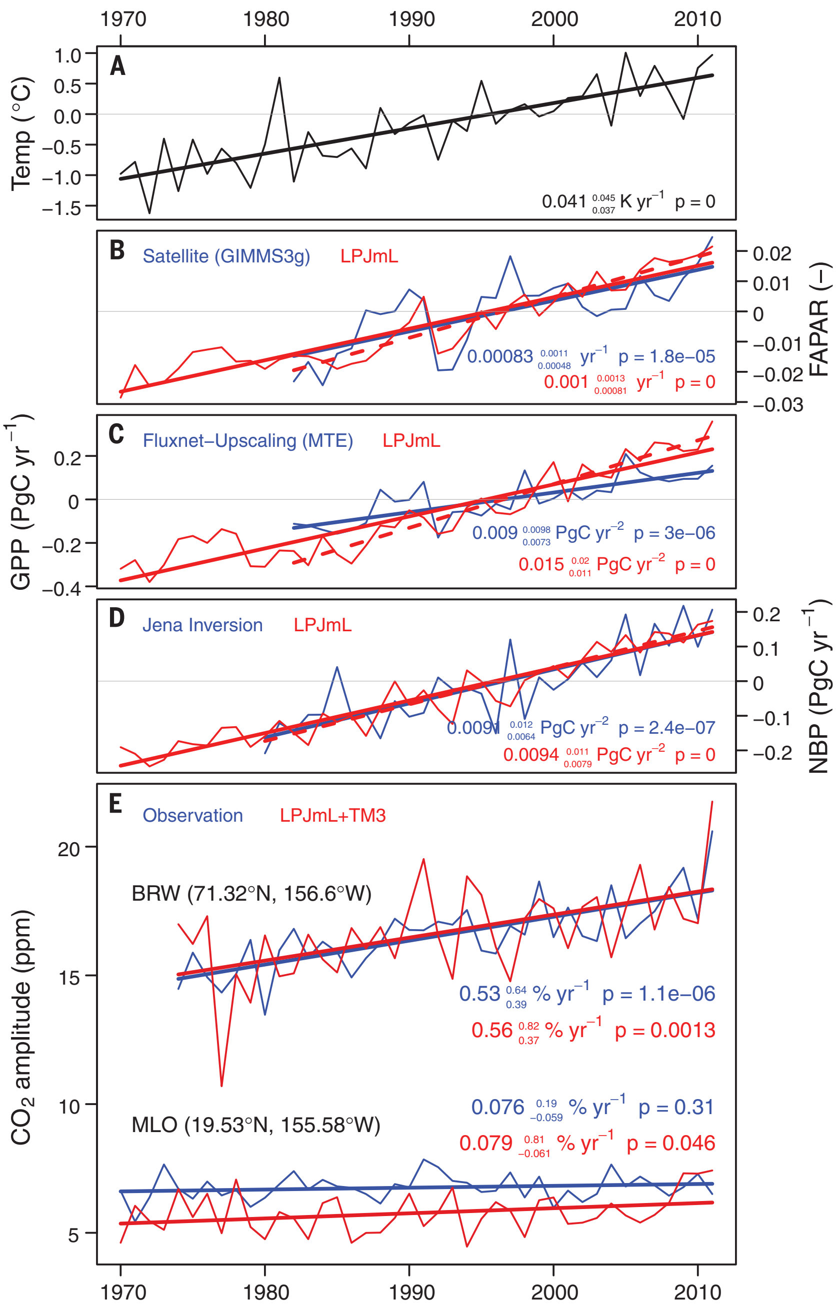

Fig. 1. Amplification of plant activity in the northern biosphere. (**A** to **E**) Annual time series and linear trends of mean annual air temperature (A), peak FAPAR (fraction of absorbed photosynthetic active radiation) (B), annual amplitude of GPP (gross primary production) (C), annual amplitude of NBP (net biome productivity) (D), and seasonal amplitude of atmospheric CO_2 (E) at Point Barrow (BRW) and Mauna Loa (MLO). Time series in (A) and (B) are spatially averaged; in (C) and (D) they are aggregated for boreal and arctic land regions north of 41°N (fig. S12), and the 1982–2011 mean has been subtracted. Dashed lines and trend values refer to the overlapping period of LPJmL simulations and observations. P values were calculated with the Mann-Kendall trend test.

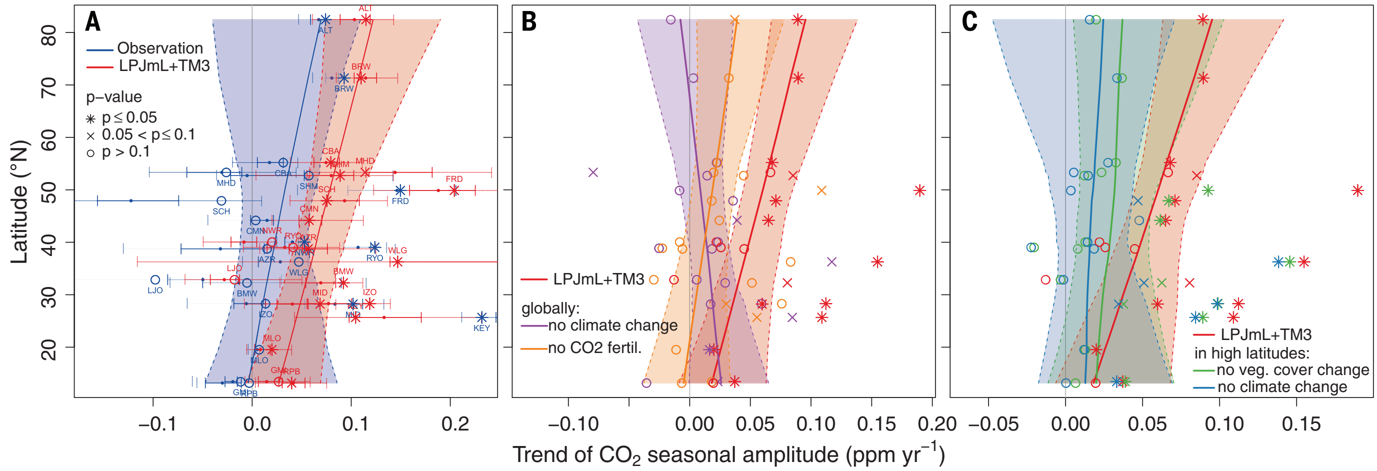

Fig. 2. Latitudinal gradients of trends in the seasonal CO_2 amplitude and its drivers. (**A**) Simulated and observed CO_2 amplitude trends with 95% confidence intervals (dashed lines) and the uncertainty distribution of site-level trend slopes (solid lines are interquartile range; dots are median values). Site-level uncertainty distributions are not shown in (B) and (C) for clarity. (**B**) Global effects of CO_2 fertilization and climate change on the latitudinal gradient. Removing the effect of CO_2 fertilization on photosynthesis reduces CO_2 amplitude trends globally but has no effect on the latitudinal gradient. The latitudinal gradient disappears with a constant climate. (**C**) Separation of the indirect effect of changing vegetation cover and the direct effect of climate change on photosynthesis in high-latitude regions on the latitudinal gradient. The latitudinal gradient disappears both without changes in vegetation cover (i.e., climate change but no vegetation cover change) and without climate change (i.e., forcing changes in vegetated area but no climate change).

two model experiments with LPJmL in which we kept temperature and precipitation at 1965–1975 levels for the period 1970–2011 (i.e., no climate change) and held CO_2 constant at 325.7 ppm after 1970 to quantify the effect of CO_2 fertilization (Fig. 2B). We found that both climate change and CO_2 fertilization affect CO_2 amplitude trends, but with regional differences: Climate change was the dominant factor on CO_2 amplitude trends north of 40°N, whereas CO_2 fertilization was the dominant factor south of 40°N. Without the effect of CO_2 fertilization, CO_2 amplitude trends were generally lower (~ −0.04 ppm $year^{-1}$ across all latitudes) but the latitudinal gradient of stronger CO_2 amplitude trends in northern relative to southern latitudes was not affected. However, the strong CO_2 amplitude trends in northern latitudes disappeared under constant climate and reverted the latitudinal gradient toward stronger trends south of 40°N (Fig. 2B). Therefore, the stronger CO_2 amplitude trends at northern latitudes are mainly dominated by climate change–induced increases in boreal and arctic GPP (Fig. 3). Increasing GPP results in increasing plant growth, which again enhances GPP. LPJmL simulates an increasing coverage of trees across the boreal zone at the expense of tundra (*23*).

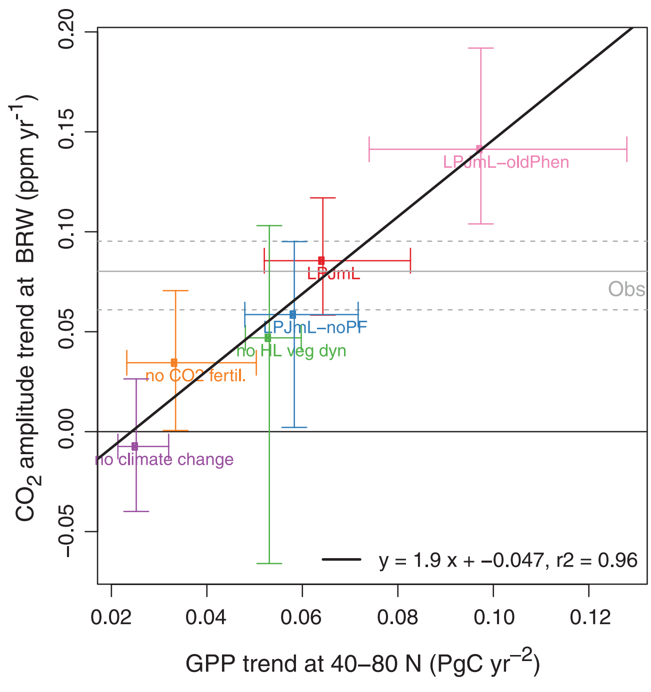

Fig. 3. Trend in the CO_2 amplitude at Point Barrow against trends in northern ecosystem gross primary production across different factorial model experiments with LPJmL. Dots and error bars represent median values and 95% confidence intervals of the estimated trends. Gray horizontal solid and dashed lines show the median and 95% confidence interval for the estimated trend in the observed CO_2 amplitude time series.

To quantify the role of this indirect vegetation cover feedback on GPP and CO_2 amplitude trends, we performed two more model experiments. In the first, we again fixed climate during the period 1970–2011 according to the climate conditions in 1965–1975 but prescribed changes in vegetated area as simulated in the standard experiment (i.e., changes in vegetation cover but no climate change). In the second, we used observed climate but fixed vegetated area after 1970 (i.e., constant vegetation cover with climate change). Both experiments were performed only for northern ecosystems; the rest of the world was simulated following the normal simulation protocol. The latitudinal gradient of stronger CO_2 amplitude trends in northern latitudes disappeared both without the direct effect of climate change and without the indirect effect of changing vegetation cover in northern ecosystems (Fig. 2C). Thus, the interaction between the direct climate effects on photosynthesis and the indirect effect of changing vegetation cover drives the trend in the CO_2 amplitude.

The climate effect is likely mostly exerted via temperature, given earlier results from eddy covariance sites, indicating that variability in ecosystem GPP north of 42°N is driven by temperature (*31*). Additional processes, such as increasing plant available water from enhanced seasonal thawing of permafrost soils and changes in plant phenology, contribute to plant productivity in northern ecosystems. Indeed, we found weaker GPP and CO_2 amplitude trends in a LPJmL simulation without considering permafrost dynamics (*24*) (LPJmL-noPF in Fig. 3) and overestimated observed GPP and CO_2 amplitude trends with a too-simplistic phenology model that only accounts for temperature effects but ignores radiation and hydrological effects on seasonal leaf development (*26*) (LPJmL-oldPhen in Fig. 3). These examples demonstrate a strong but complex control of climate on plant productivity in northern ecosystems, which ultimately results in the major contribution of enhanced plant growth to the strong CO_2 amplitude trends in northern latitudes.

Our results suggest that a major driver of the large increase in CO_2 amplitude at high northern latitudes involves the interaction of recent climate change with vegetation dynamics. Climate change affects processes such as plant physiology, phenology, water availability, and vegetation dynamics, ultimately leading to increased plant productivity and vegetation cover in northern ecosystems in recent decades. Our results further highlight the gradual replacement of herbaceous vegetation with forests as a major specific factor. Lastly, we identified a dominance of changes in photosynthesis over respiration in driving the changes. Sensitivities of these processes to climate need to be carefully assessed in current ecosystem and Earth system models against observational data to accurately reproduce observed changes in CO_2 amplitude. However, the stimulation of photosynthesis and vegetation growth by climate change cannot be unlimited because of nutrient limitations, radiation, and possibly increased mortality (*32*). Thus, at some point in the future, the positive trends in plant productivity (and thus the CO_2 amplitude increase) might stall. Continued long-term observation of atmospheric CO_2, together with ground and satellite observations of vegetation productivity and dynamics, will be the key to detection, modeling, and better prediction of such changes in high-latitude carbon cycle dynamics.

REFERENCES AND NOTES

1. C. D. Keeling, J. F. S. Chin, T. P. Whorf, *Nature* **382**, 146–149 (1996).
2. J. T. Randerson, M. V. Thompson, T. J. Conway, I. Y. Fung, C. B. Field, *Global Biogeochem. Cycles* **11**, 535–560 (1997).
3. R. B. Bacastow, C. D. Keeling, T. P. Whorf, *J. Geophys. Res.* **90**, 10529–10540 (1985).
4. H. D. Graven *et al.*, *Science* **341**, 1085–1089 (2013).
5. M. Heimann, C. D. Keeling, C. J. Tucker, in *Aspects of Climate Variability in the Pacific and the Western Americas*, D. H. Peterson, Ed. (American Geophysical Union, Washington, DC, 1989), pp. 277–303.
6. IPCC, *Climate Change 2013—The Physical Science Basis: Working Group I Contribution to the Fifth Assessment Report of the Intergovernmental Panel on Climate Change* (Cambridge Univ. Press, 2014).
7. R. B. Myneni, C. D. Keeling, C. J. Tucker, G. Asrar, R. R. Nemani, *Nature* **386**, 698–702 (1997).
8. W. Lucht *et al.*, *Science* **296**, 1687–1689 (2002).
9. I. H. Myers-Smith *et al.*, *Environ. Res. Lett.* **6**, 045509 (2011).
10. L. T. Berner, P. S. A. Beck, A. G. Bunn, S. J. Goetz, *Glob. Change Biol.* **19**, 3449–3462 (2013).
11. P. S. A. Beck *et al.*, *Glob. Change Biol.* **17**, 2853–2866 (2011).
12. M. Jung *et al.*, *J. Geophys. Res.* **116**, G00J07 (2011).
13. A. Anav *et al.*, *Rev. Geophys.* **53**, 785–818 (2015).
14. C. Rödenbeck, S. Houweling, M. Gloor, M. Heimann, *Atmos. Chem. Phys.* **3**, 1919–1964 (2003).
15. J. M. Gray *et al.*, *Nature* **515**, 398–401 (2014).
16. N. Zeng *et al.*, *Nature* **515**, 394–397 (2014).
17. J. Barichivich *et al.*, *Glob. Change Biol.* **19**, 3167–3183 (2013).
18. N. MacBean, P. Peylin, *Nature* **515**, 351–352 (2014).
19. Z. Zhu *et al.*, *Remote Sens.* **5**, 927–948 (2013).
20. S. Sitch *et al.*, *Glob. Change Biol.* **9**, 161–185 (2003).
21. A. Bondeau *et al.*, *Glob. Change Biol.* **13**, 679–706 (2007).
22. M. Heimann, S. Körner, "The global atmospheric tracer model TM3," *Tech. Rep. Max Planck Inst. Biogeochem. 5* (2003), p. 131.
23. See supplementary materials on *Science* Online.
24. S. Schaphoff *et al.*, *Environ. Res. Lett.* **8**, 014026 (2013).
25. K. Thonicke *et al.*, *Biogeosciences* **7**, 1991–2011 (2010).
26. M. Forkel *et al.*, *Biogeosciences* **11**, 7025–7050 (2014).
27. M. Forkel *et al.*, *Glob. Change Biol.* **21**, 3414–3435 (2015).
28. M. Reichstein *et al.*, *Nature* **500**, 287–295 (2013).
29. C. Beer *et al.*, *Science* **329**, 834–838 (2010).
30. R. J. Norby *et al.*, *Proc. Natl. Acad. Sci. U.S.A.* **102**, 18052–18056 (2005).
31. M. Reichstein *et al.*, *Geophys. Res. Lett.* **34**, L01402 (2007).
32. S. Trumbore, P. Brando, H. Hartmann, *Science* **349**, 814–818 (2015).

ACKNOWLEDGMENTS

We thank the following institutions and scientists that acquired and provided CO_2 site data: E. Dlugokencky (NOAA), Scripps Institution of Oceanography, D. Worthy (Environment Canada), F. Meinhardt (Umweltbundesamt), R. Langenfelds and P. Krummel (CSIRO), and H. Koide (JMA). We further thank the following groups, institutions, or scientists for sharing their data sets: AFS, CRU, EC/JRC, ECMWF, GIMMS, NCEP, NRCan, L. Giglio (UMD), M. Jung (MPI-BGC), and S. E. Mikaloff Fletcher (National Institute of Water and Atmospheric Research). We thank S. Schaphoff (PIK) for comments on LPJmL and I. C. Prentice and R. Thomas for comments on the manuscript. Supported by the European Union (FP7) through the projects GEOCARBON (283080), CARBONES (242316), and EMBRACE (283201); U.S. Department of Energy grant DE-SC0012167; NSF grant 1304270; and NOVA grant UID/AMB/04085/2013. Table S7 provides an overview of used data and how it can be obtained. Results from factorial model experiments with LPJmL+TM3 are available at http://doi.pangaea.de/10.1594/PANGAEA.856722.

SUPPLEMENTARY MATERIALS

www.sciencemag.org/content/351/6274/696/suppl/DC1
Materials and Methods
Supplementary Text
Figs. S1 to S13
Tables S1 to S7
References (*33*–*69*)

4 May 2015; accepted 11 January 2016
Published online 21 January 2016
10.1126/science.aac4971

GLOBAL WATER CYCLE

A decade of sea level rise slowed by climate-driven hydrology

J. T. Reager,[1]* A. S. Gardner,[1] J. S. Famiglietti,[1,2] D. N. Wiese,[1] A. Eicker,[3] M.-H. Lo[4]

Climate-driven changes in land water storage and their contributions to sea level rise have been absent from Intergovernmental Panel on Climate Change sea level budgets owing to observational challenges. Recent advances in satellite measurement of time-variable gravity combined with reconciled global glacier loss estimates enable a disaggregation of continental land mass changes and a quantification of this term. We found that between 2002 and 2014, climate variability resulted in an additional 3200 ± 900 gigatons of water being stored on land. This gain partially offset water losses from ice sheets, glaciers, and groundwater pumping, slowing the rate of sea level rise by 0.71 ± 0.20 millimeters per year. These findings highlight the importance of climate-driven changes in hydrology when assigning attribution to decadal changes in sea level.

Over the past century, sea level rose at an average rate of 1.5 ± 0.2 mm $year^{-1}$, increasing to 3.2 ± 0.4 mm $year^{-1}$ during the past two decades (*1*). The increase in the rate of rise is attributed to an increase in mass loss from glaciers and ice sheets and to ocean warming. Although these contributions are fairly well constrained, trends in sea level also contain a land water storage component that is acknowledged to be among the most important yet most uncertain contributions (*1*–*3*), in which land water storage is defined by the Intergovernmental Panel on Climate Change (IPCC) (*1*) as all snow, surface water, soil moisture, and groundwater storage, excluding glaciers. Every year, land temporarily stores then releases a net 6000 ± 1400 Gt of mass through the seasonal cycling of water, which is equivalent to an oscillation in sea level of 17 ± 4 mm (*4*–*6*). Thus, natural changes in interannual to decadal cycling and storage of water from oceans to land and back can have a large effect on the rate of sea level rise (SLR) on decadal intervals (*7*, *8*). From 2003 to 2011, SLR slowed to a rate of ~2.4 mm $year^{-1}$ (*9*) during a period of increased mass loss from glaciers (*10*) and ice sheets (*11*). Climate-driven changes in land water storage have been suggested to have contributed to this slowdown (*9*), but this assertion has not been verified with direct observations.

Until recently, little data have existed to constrain land water storage contributions to global

[1]Jet Propulsion Laboratory, California Institute of Technology, CA, USA. [2]Department of Earth System Science, Department of Civil and Environmental Engineering, University of California, Irvine, CA, USA. [3]Institute of Geodesy and Geoinformation, University of Bonn, Bonn, Germany. [4]Department of Atmospheric Sciences, National Taiwan University, Taipei, Taiwan.
*Corresponding author. E-mail: john.reager@jpl.nasa.gov

Science

Enhanced seasonal CO_2 exchange caused by amplified plant productivity in northern ecosystems

Matthias Forkel, Nuno Carvalhais, Christian Rödenbeck, Ralph Keeling, Martin Heimann, Kirsten Thonicke, Sönke Zaehle and Markus Reichstein

Science **351** (6274), 696-699.
DOI: 10.1126/science.aac4971originally published online January 21, 2016

Warming making bigger CO_2 swings
The combined effects of climate change and vegetation dynamics at high northern latitudes have amplified the seasonal variation of atmospheric CO_2 concentrations over the past half century. Forkel *et al.* combined observations and models to show that climate warming has caused the photosynthetic uptake of carbon to increase faster than its respiratory release from the terrestrial biosphere. This has increased the difference from summer to winter, as well as the latitudinal gradient. Because of the physiological limitations to carbon uptake by terrestrial vegetation, this negative feedback to warming in the boreal north and Arctic cannot continue indefinitely.
Science, this issue p. 696